IOPscience iopscience.iop.org

Home Search Collections Journals About Contact us My IOPscience

Transport in a superlattice of 1D ballistic channels

This article has been downloaded from IOPscience. Please scroll down to see the full text article.

1990 J. Phys.: Condens. Matter 2 3405

(http://iopscience.iop.org/0953-8984/2/14/025)

View the table of contents for this issue, or go to the journal homepage for more

Download details:
IP Address: 171.66.16.103
The article was downloaded on 11/05/2010 at 05:51

Please note that terms and conditions apply.

J. Phys.: Condens. Matter **2** (1990) 3405–3414. Printed in the UK

LETTER TO THE EDITOR

Transport in a superlattice of 1D ballistic channels

C G Smith†, M Pepper†, R Newbury†, H Ahmed†, D G Hasko†, D C Peacock†, J E F Frost†, D A Ritchie†, G A C Jones† and G Hill‡

† Cavendish Laboratory, Madingley Road, Cambridge CB3 0HE, UK

‡ Department of Electrical Engineering, The University of Sheffield, Mappin Street, Sheffield S10 2TN, UK

Received 6 November 1989, in final form 7 February 1990

Abstract. We have fabricated a 2D array of 1D narrow channels in a square lattice configuration on a high mobility GaAs/GaAlAs heterostructure. When a gate voltage is applied the underlying two-dimensional electron gas is depleted creating 4000 dots, of size 0.2 μm, leaving a grid-like conducting path of quasi one-dimensional channels that are linked every 0.5 μm. For low values of magnetic field the Hall voltage measured on either side of the device is quenched across its entire width of 25 μm. The longitudinal magneto-resistance reveals Aharonov–Bohm oscillations with a flux period of h/e for magnetic fields up to 0.4 T. The conductance versus gate voltage shows structure that is consistent with Bragg reflections of the electron waves when the one-dimensional subband wavelength at the Fermi energy, in the direction of current flow, is equal to one superlattice period. Dips in the conductance when this criteria is met show a ln T temperature dependence, similar in origin to a 2D quantum interference. A magnetic field quenches these dips when the cyclotron orbit is comparable with the superlattice period.

We have investigated a device that applies a superlattice potential to a two-dimensional electron gas (2DEG) via a patterned gate consisting of squares of side 0.2 μm with a centre to centre separation of 0.5 μm. The 2DEG is created at the interface of a GaAs/GaAlAs heterostructure which is 70 nm below the patterned gate. When a negative gate voltage is applied the carriers are depleted under the square dots resulting in a grid-like conducting structure of 0.5 μm long 1D ballistic channels connected both in parallel and series. The unit cell of such a device is a combination of two structures already realised; in one direction it resembles the two ballistic 1D channels in series investigated by Wharam *et al* [1], and in the other it resembles the two ballistic 1D channels in parallel measured by Smith *et al* [2].

The device was fabricated in the manner developed by Ford *et al* [3] using electron beam lithography to pattern a polymethylmethacrylate layer 100 nm thick as a dielectric on the surface of the heterostructure, over which Au was evaporated from three different directions at an angle of 45 degrees to a thickness of 200 nm. The pattern of 4000 repeated squares was defined on a 25 μm wide Hall bar over a length of 40 μm. The superlattice region was connected to the wide 2D region at each end via a 5 μm long and 5 μm wide

0953-8984/90/143405 + 10 $03.50 © 1990 IOP Publishing Ltd

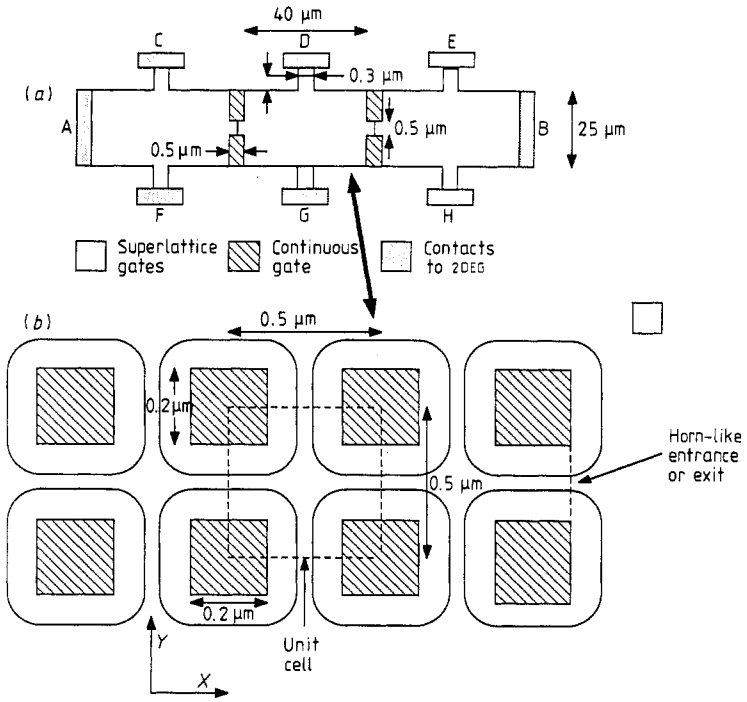

Figure 1. (*a*) The shape of the gate pattern on the Hall bar is shown and the position of the various contacts is marked. (*b*) A close up of the shaded area in (*a*) of the superlattice showing the shape of the gates and the effect of depletion. A unit cell is marked.

Table 1. The device parameters for the two samples.

Device	Period, a (nm)	Mobility, μ (cm V^{-1} s^{-1})	Carrier concentration, n (cm^{-2})	Comments
No 1	0.5	8.3×10^5	3.2×10^{11}	No Hall probes. Larger dot size
No 2	0.5	1.21×10^6	3.2×10^{11}	Hall probes. Smaller dot size

opening in the gate metallisation. Two Hall probes 4 μm wide were in contact with each side of the superlattice region (figure 1).

The two devices studied had nominally the same shape, but were fabricated on differing substrates with the same underlying layer structure which was as follows: a superlattice buffer [(AlAs 2.4 nm, GaAs 2.5 nm) $\times$ 25] was grown first on a semi-insulating substrate, followed by 1 μm of nominally undoped GaAs. On top of this, 20 nm of undoped AlGaAs was grown, followed by 40 nm of AlGaAs (Si doped at 10^{18} cm^{-3}) and topped by a 10 nm undoped GaAs capping layer. The resulting characteristics are shown in table 1.

All the measurements in this paper were performed in a dilution refrigerator over a temperature range, 30–500 mK. The sample was operated in the regime where the

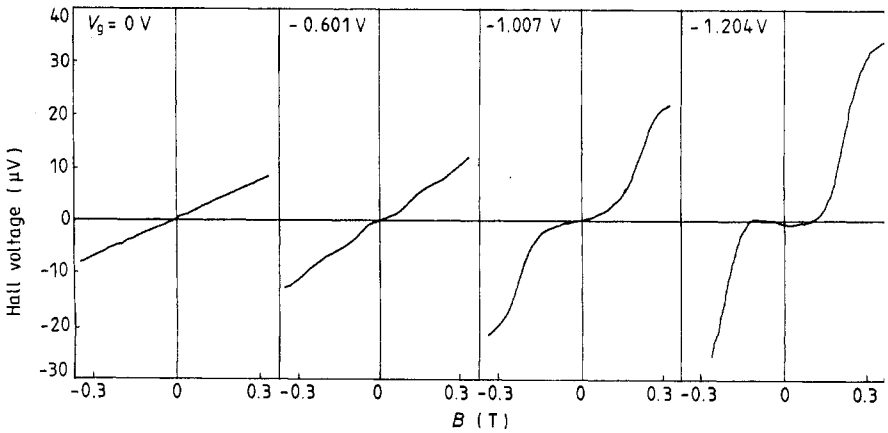

Figure 2. A plot of the Hall voltage in sample 2 measured off contacts D and G, with a current applied to contacts A and B. The Hall voltage is plotted for four different gate voltages.

carriers have been depleted from underneath the gated squares. We do not consider the case of low negative gate voltages, which was recently investigated in a similar structure by Alves *et al* [4], but instead we have studied the large negative gate voltage case when the current flows around the superlattice of dots. Changing the gate voltage in this regime changes the depletion width around each dot simultaneously. This provides a weak 1D periodic potential of period 0.5 μm in the direction of the current flow, as the periodic change in channel width causes a periodic change in the energy of the 1D subbands confined between the dots. The quasi-1D nature of this device should enhance the amplitude of any superlattice effects [5]. Our reasons for describing the channels as weakly coupled will be discussed.

In figure 2 we show Hall voltage measurements, while in figure 3(*a*) we show the variation in conductance of sample 2, measured in two different orientations, as the gate voltage was changed. Figure 3(*a*) is for voltages measured between contacts C and E when the current was applied to contacts A and B. The structure which can clearly be seen in these curves will be discussed shortly. First we will show how the Hall voltage measurements of figure 2 support our claim that this sample closely resembles weakly coupled 1D channels. In this figure the Hall voltage is plotted against the magnetic field for four different gate voltages and as can be seen, as well as the carrier concentration dropping with gate voltage there is a low field quench of the Hall voltage across the 25 μm wide Hall bar. The carriers are depleted under the 0.2 μm wide squares when $V_g = -0.55$ V, but the Hall voltage is quenched for a gate voltage range from $V_g = -1$ V to pinch off at -1.32 V. Such quenches in the Hall voltage have been seen before in single narrow 1D channels with small closely spaced Hall probes [6, 7]. The existence of this quench implies that at fields below 0.15 T the electrons are preferentially focused from the exit of the 1D channel defined by one pair of dots into the channel defined by the next pair. This follows the most recent theoretical explanation for the quenching of the Hall effect which is given in [8], where the idea of electron collimation from the horn like entrances and exits from the 1D channels is proposed. Other workers have explained the quenching in quantum mechanical terms [9] without invoking collimation effects. The two-terminal magneto-resistance measured through contacts D and G is displayed in figure 4. The zero-field peak results from localisation in the contacts and is the same

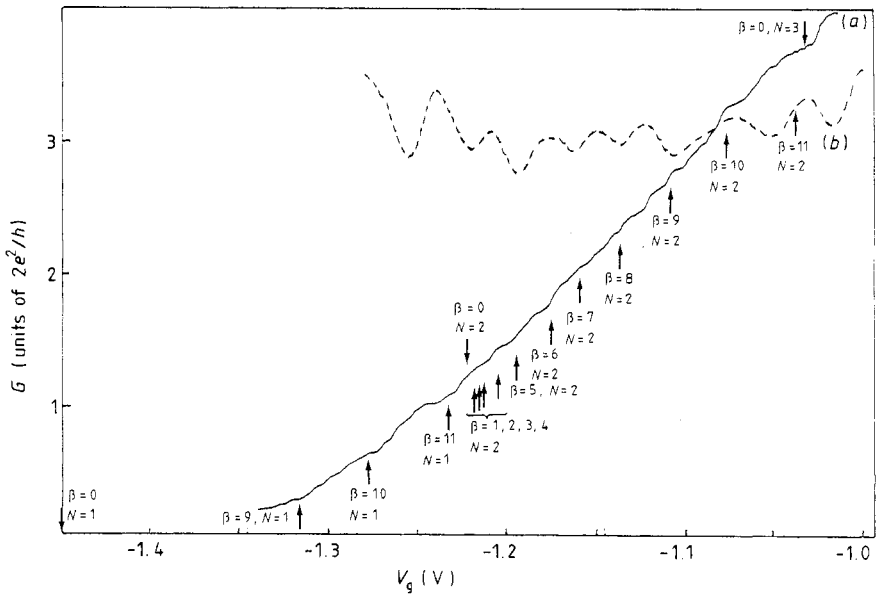

Figure 3. A graph of conductance against gate voltage for sample 2. Curve (*a*) is a four-terminal measurement with currents in contacts A and B and voltage measured off contacts C and E. The top arrows mark the gate voltage for which equation (4) is valid for $N = 1, 2$ and $N = 3$. The bottom arrows mark the gate voltage for which equation (7) is valid for $n =$ 1 and 2 and for $\beta = 1, 2, 3$ and 4. Curve (*b*) is a plot of the differential of curve (*a*) with arbitrary units in the vertical direction. The width w between the dots in this direction varies as $w = (217 + 114V_g)$nm.

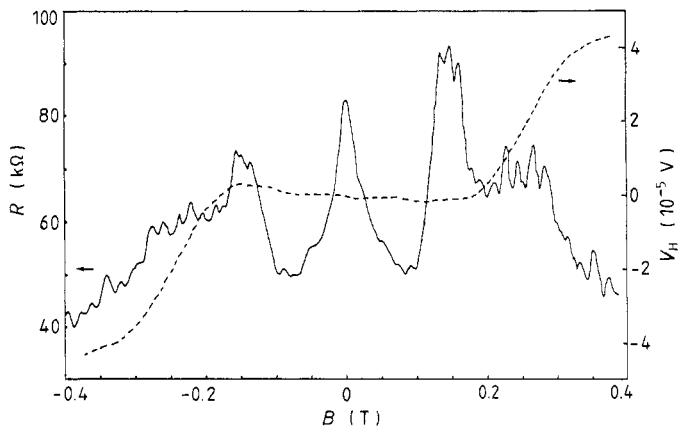

Figure 4. The full trace is a plot of the two-terminal magneto-resistance applied to contacts D and G for a gate voltage of −1.3 V. The broken trace marks the Hall voltage for the same gate voltage measured off contacts D and G with current applied to contacts A and B.

for $V_g = 0$, but the large peak that appears at fields just below those at which the quench disappears becomes larger as the gate voltage is made smaller. The small periodic oscillations superimposed on this background resistance have a period of 0.051 T.

Surprisingly for a large array of circles, as exists in this case, these oscillations appear to be Aharonov–Bohm oscillations occurring every time a flux of h/e fits within a circle of diameter 0.32 μm. One would expect the h/e oscillations to be averaged out as each oscillation associated with each ring will have a random phase compared to any other (the reversed path $h/2e$ oscillations would normally be expected at low fields when the magnetic length $(h/eB)^{1/2}$ is longer than the circumference, which in this case corresponds to 0.01 T). The oscillations we observe occur for fields from 0.08 T up to 0.4 T when the current begins to be confined to edge states. Perhaps because all the dots are surrounded by a current rotating in edge states in the same direction around dots of the same circumference, with no impurity scattering to provide random phase variations between each dot, the oscillations appear in phase.

At high magnetic fields when the cyclotron orbit is smaller than the 1D channel widths, the Hall voltage is quantised as in a large 2DEG. (For channels 30 nm wide, B must be greater than 3 T.) The Hall effect for fields greater than 2–3 T was linear and can be used to deduce the carrier concentration variation with gate voltage. Only sample 2 had working Hall probes allowing a measurement of the variation of n with V_g giving:

$$n = (3.51 + 2.02V_g) \times 10^{15}\ \mathrm{m}^{-2} \tag{1}$$

for $-1.25\mathrm{V} < V_g < -0.25\mathrm{V}$.

To investigate how the width, w, of the conducting channel between the depleted dots changes with gate voltage we use the fact that when the 2DEG is just depleted under the dots the conducting width has the lithographically defined value of 0.3 μm minus twice the separation of the gates from the 2DEG (2×0.07 μm) [10]. We also know that the device pinches off when the conductance goes to zero and the conductance versus gate voltage is close to linear, differing only near pinch-off. The variation of w with V_g is discussed in the figure captions for figure 3. The gate pattern of each dot resembles the single dot already studied for two ballistic channels in parallel patterned on the same material. The voltage at which the dots just deplete the 2DEG under them (-0.5 V) and the voltage at which the channels between the dots are pinched off are similar in both types of device. In the case of the single dot the variation of the depletion width with gate voltage was measured using the Aharonov–Bohm effect, and it was found to fit to within 10% with that calculated from using the simple method of estimating w we have used above. From equation (1) we also know the carrier concentration variation with gate voltage so the conductance is given by

$$G = wne\mu P/L$$

where P is the number of dots perpendicular to the current flow and L is the length of the superlattice. Experimentally the mobility μ in a 2DEG is known to vary with n as [11]

$$\mu \propto n^{3/2} \tag{2}$$

for a large 2DEG. This enables us to calculate w for a given gate voltage. Interestingly the measured conductance is three times that calculated by assuming that if there are N 1D subbands between each dot then the total conductance will be given by:

$$G = (W/L)(2e^2/h)N \tag{3}$$

where W = the width of the mesa, L = the length of the superlattice and $N = wK_f/\pi$. Which is what would be expected for a grid-like resistor network with each resistor consisting of a quantised ballistic conductor of width w. Equation (3) is the value of G one would expect if each constriction between each pair of dots acted as an independent

resistor. In fact these results show that three resistors added together have the same resistance as one on its own, which is further evidence for the non-addition of resistors in the ballistic regime when the electrons pass through the resistors without scattering [1]. The implication is that at $V_g = -1$ V the electrons traverse three superlattice periods (1.5 μm) before they are scattered, this corresponds to a mobility of $\mu = 250\,000\ \mathrm{cm^2\,V^{-1}\,s^{-1}}$. In a large 2DEG without the dots one would expect a reduction of the mobility to $\mu = 300\,000\ \mathrm{cm^2\,V^{-1}\,s^{-1}}$ due to the variation in carrier concentration (from equation (2)), which is close to that deduced from assuming that the electrons traverse three superlattice periods without scattering. In other words the scattering in the superlattice is dominated by random impurities and the addition of the dots has not introduced any new mechanism.

Due to misalignment during the exposure, the pattern of dots in both samples extends 4 μm over the Hall probe on one side (see figure 1), which means that the resistance through contacts D and G is 1.62 R_0, where R_0 is the average reistance per square of the lattice. Coincidentally this is the same as for the four-terminal resistance measured from the source to the drain. In addition the fact that the pinch-off voltages differ by 50 mV for sample 2 when measured in the two orthogonal directions X and Y implies that, due to processing errors, the two orthogonal sides of the squares differ in length by 100 nm.

Differentiation of curve (*a*) in figure 3 reveals a great deal of structure in the turn off characteristics (see curve (*b*) in figure 3). The differentiation was carried out after numerically filtering the data with a high pass filter set at 40 $\mathrm{V^{-1}}$. This smooths the data and removes some of the structure due to noise, and leads to a broadening of the peaks by 25 mV. Such a value was chosen because it corresponds to the uncertainty in V_g due to thermal broadening which is calculated from

$$\mathrm{d}w = (w/2)(k_B T/E_f)^{1/2}.$$

We know how E_f and w vary with V_g so we can calculate how the temperature relates to V_g giving

$$\mathrm{d}V_g = 80T^{1/2}\ \mathrm{mV}.$$

At first it is tempting to assign this structure to the removal of one-dimensional subbands as the channel width is narrowed, particularly if each channel loses a subband at the same voltage. (Previous measurements on two 1D channels 0.2 μm long by 0.3 μm wide separated by 0.5 μm revealed that even if the channels differ slightly in width there is evidence to suggest that the subbands in the different apertures depopulate at the same voltage [2].) Using equations (1) and (2) the gate voltage at which the N_{th} subband depopulates can be calculated, by noting for what values of V_g, $E_F = E_N$, where E_F is the Fermi energy and E_N is the energy of the Nth subband. Considering the potential to be square well like, which is reasonable so long as $w > 50$ nm [12], then equating E_F with E_N gives

$$2nw^2/\pi = N^2. \tag{4}$$

After solving equation (4) numerically for $N = 1$, 2 and 3 the various values of V_g are obtained. These are marked on figure 3 and show that this cannot explain all the structure in the pinch-off characteristics. It is reassuring to note that the average plateau separation in the gate voltage for the two 1D channels in parallel [2] (which was defined on the same material) is 0.2 V, while that calculated from equation (3) is 0.18 V. The extra structure

in figure 3 implies the existence of mini bands, and Bragg reflections, resulting from the periodic potential in the direction of current flow.

The potential in the x direction is of the form $V(x) = V(x + a)$, which results in a standing wave whenever

$$\beta\gamma_{FN} = 2a \qquad \beta = 1, 2, 3 \ldots \tag{5}$$

where λ_{FN} is the electron wavelength for the Nth 1D subband at the Fermi energy (which is given by $\lambda_{FN} = 2\pi/(kf - \pi N^2/w^2)^{1/2}$), and a, is the superlattice period. The Schrödinger equation can be solved using the Fourier transform of the periodic function $V(x)$ in a matrix equation [13]. The width of the βth band gap is proportional to the βth Fourier component of V_g. For a perfect sine potential a gap will only open for $\beta = 1$. In samples 1 and 2 the potential should be similar to a square well potential with a smooth transition from the maximum to the minimum over a range of 0.15 μm. The potential is related to the Nth 1D subband by

$$V(x) = (h^2/2m^*)(N\pi/w(x))^2 \tag{6}$$

where $w(x)$ is the variation in the channel width in the y direction as x is varied. Thus the higher energy 1D subbands will be affected to the greatest extent by the potential. The structure in the conductance versus gate voltage curves will not only be seen if a gap develops in the conduction band but it will also be seen when the group velocity, $v_N(k)$, varies where

$$v_N(k) = (1/h)(\delta E(k)/\delta k_N).$$

In addition the probability of scattering will alter with V_g. The scattering will be at a maximum and the group velocity will be at a minimum when equation (4) is satisfied. To find the values of gate voltage at which structure due to Bragg reflection will be seen we must modify equation (4) to get

$$2nw^2/\pi - (\beta w/a)^2 = N^2. \tag{7}$$

The values of V_g obtained from equation (7) are marked on figure 3 showing a reasonable fit to the peaks in the differential of V_g against G. The lower index bands are separated from each other by less than 25 mV in the gate voltage. Due to temperature broadening these bands are not revealed. Although the peaks do not fit the structure in the conductance versus gate voltage curves exactly, they do explain why over this range of gate voltages there are more than six dips when there should only be two due to the 1D subbands being depopulated. There is a reasonable correlation between the measured structure and that predicted due to Bragg reflections, considering the assumptions involved.

In figure 5 the conductance is plotted against gate voltage for five temperatures from 32 mK to 480 mK for sample 1. The structure is very much more dramatic with sharp dips in conductance at specific values of V_g. These measurements were taken two terminally as there were no Hall probes on this sample. The inset shows the temperature dependence of the dips plotted against ln T showing a similar slope. The change in conductivity is given by

$$\partial\sigma = 0.03(e^2/h) \ln T. \tag{8}$$

The resemblance to 2D localisation will be explained subsequently. Although sample 1 was fabricated on a similar substrate to sample 2, with the same initial carrier concentration (see table 1), the final pinch-off was at a more negative gate voltage of

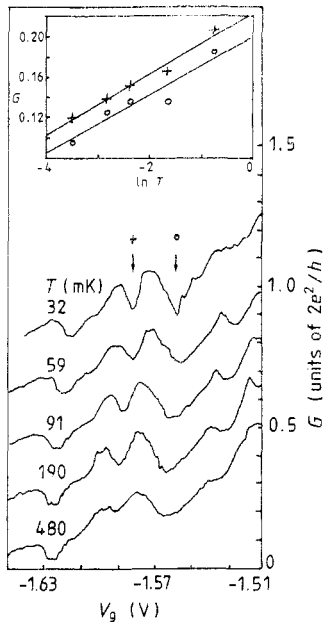

Figure 5. A plot of the conductance versus gate voltage for sample 1 at five different temperatures. The current and voltage were applied to contacts D and G. The curves are offset by (0.2) $2e^2/h$ for clarity. The inset shows a plot of peaks 2 and 3 plotted against $\ln T$; +: $G = (0.20 + 0.38 \ln T)$; ○: $G = (0.23 + 0.03 \ln T)$. Due to a slight hysteresis in the resistance versus gate voltage curves, some of the peaks have different positions of gate voltage. This is just a shift in the whole curve to either higher or lower gate voltages.

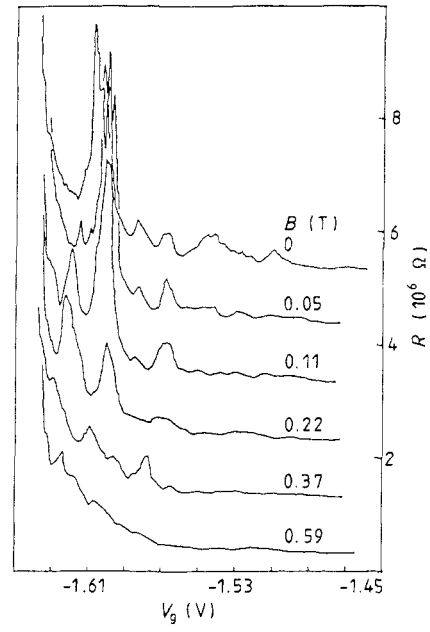

Figure 6. A plot of the resistance of sample 2 against gate voltage with the current and voltage as in figure 5. Each of the six curves were measured with a different magnetic field applied perpendicular to the 2DEG. The curves are offset by 1 MΩ for clarity.

−1.625 V. This would imply that the 1D channels were wider by approximately one third. The distribution of the positions of the peaks in figure 5 for sample 1 are similar to those of curve B in figure 3 for sample 2, with the average peak separation of sample 2 being 50 mV while that for sample 1 is 45 mV. This is evidence that the structure has the same cause.

The fact that the dips in the conductance follow the behaviour of weak 2D localisation can be explained if we assume that the electrons are localised when the Bragg reflection condition is satisfied. This is not a result of disorder, but occurs because the transmission coefficient, T_i, for an electron encountering a superlattice potential goes to zero at the Bragg condition, while at other energies T_i remains close to 1 and the electron wavefunction is an extended Bloch wave. At the Bragg reflection condition the electron is partially reflected by T_i every time it encounters a double barrier, so its amplitude is reduced by T_i^M when it has traversed M superlattice periods. This provides an exponential envelope function to any initially free electron wave packet, localising the wavefunction over a range such that $T_i^M < 0.5$ or

$$M < -0.7/\ln T_i \tag{9}$$

this leads to a localisation length, L_{Loc} given by

$$L_{Loc} = 2Ma = -0.7/\ln T_i \,\mu m. \tag{10}$$

If $T_i = 0.8$ then $L_{Loc} = 3\,\mu m$. As the temperature is increased the phase breaking length L_φ will be reduced until, when $L_\varphi < L_{Loc}$, the electrons will only experience weak localisation and diffusion will occur more readily. If L_φ is long enough then these dips in the conductance would go to zero leading to complete gaps in the density of states. For a different gate voltage away from the Bragg condition, T_i will be close to 1 so the localisation length will be very large and no dips in the conductance will be observed. At the Bragg condition the conductivity will thus be given by

$$\partial\sigma = 2.3(e^2/h)\ln(L_{Loc}/L_\varphi). \tag{11}$$

The localisation appears to be 2D in nature because the electrons are moving round a grid in both the x and y direction so long as L_{LOC} is larger than one superlattice period. This mechanism for removing the structure with temperature is different from the thermal activation of the electrons across the mini bands which would lead to an exponential variation of conductance with temperature. Using equation (10) the difference in magnitude of the structure in the conductance versus gate voltage between the two samples can be explained. A small change of T_i of 10% between the two samples at the Bragg condition will produce a change of L_{Loc} of 100%. This could be caused by a small difference in the exposure conditions for sample 2 such that the gate pattern has smoother features than sample 1 resulting in better focusing and therefore a larger value of T_i. As the phase breaking length should be the same in both samples the resulting features due to localisation at the Bragg condition are very much smaller in sample 2.

Figure 6 contains several plots of the resistance in sample 1 measured in a two terminal manner off contacts D and G as the gate voltage is varied. Each curve was taken at a different magnetic field perpendicular to the plane of the 2DEG. It is immediately obvious that the amplitude of the peaks is reduced as the magnetic field is increased, until at 0.59 T the majority of the structure is quenched. The structures at more negative gate voltages require larger magnetic fields to remove them. As the carrier concentration could not be measured as V_g was varied in sample 1, it had to be estimated from the behaviour of sample 2. In that sample the carrier concentration had dropped to one third of its original value by the time the device was close to pinch-off. This value was used to estimate the size of the cyclotron orbit at these magnetic fields indicating that the structure disappears when the cyclotron orbit is comparable to the superlattice period.

In conclusion we have fabricated a device containing a strong 2D superlattice potential that creates a grid-like conducting structure of period 0.5 μm. The conduction through this grid behaves like many loosely coupled 1D wires which contain a periodic potential along their length. One such device with Hall probes allows the carrier concentration to be measured as the gate voltage is varied. At low magnetic fields the Hall voltage is quenched over a distance of 25 μm, while the longitudinal resistance shows h/e Aharonov–Bohm oscillations. This is consistent with the theoretical predictions that the Landau levels are split into p sub-bands when p flux quanta are threaded through each unit cell [14]. A large broad peak in the resistance is observed at the same magnetic field as that for which the quench in the Hall voltage ends and it occurs when the cyclotron orbit is comparable to the depleted dot size. The two samples exhibit structure in the conductance as the gate voltage is varied, which is consistent with 1D subbands between

the dots showing Bragg reflections whenever the wavelength in the x direction is equal to the superlattice period. In one of the samples the dips in the conductance are large enough for their temperature dependence to be measured and compared to 2D localisation. The localisation is due to the reduction in the transmission coefficient when the Bragg condition is satisfied and reduces as the temperature is increased, because the phase breaking length for electrons also decreases with increasing temperature. A magnetic field quenches the peaks in the resistance when the cyclotron orbit becomes comparable to the superlattice period.

This work was supported by the SERC and, in part, by the European Research Office of the US Army. I would like to thank M J Kelly and T J Thornton for useful discussions.

References

[1] Wharam D A, Pepper M, Ahmed H, Frost J E F, Hasko D G, Peacock D C, Ritchie D A and Jones G A C 1988b *J. Phys. C: Solid State Phys.* **21** L887
[2] Smith C G, Pepper M, Newbury R, Ahmed H, Hasko D G, Peacock D C, Frost J E F, Ritchie D A and Jones G A C 1989 *J. Phys.: Condens. Matter* **1** 6763
[3] Ford C J B, Thornton T J, Newbury N, Pepper M, Ahmed H, Peacock D C, Ritchie D A, Frost J E F and Jones G A C 1989 *Appl. Phys. Lett.* **54** 21
[4] Alves E S, Beton P H, Henini M, Eaves L, Main P C, Hughes O H, Toombs G A, Beaumont S P and Wilkinson C D W 1989 *J. Phys.: Condens. Matter* **1** 8257
[5] Kelly M J 1986 *Surf. Sci.* **170** 49
[6] Roukes M L, Scherer A, Allen S J Jr, Craighead H G, Ruthen R M, Beeby E D and Harbison J P 1988 *Phys. Rev. Lett.* **59** 3011
[7] Ford C B J, Thornton T J, Newbury R, Pepper M, Ahmed H, Peacock D A, Frost J E F and Jones G A C 1988 *Phys. Rev.* B **38** 8518
[8] Beenakker C W J and van Houten H *Preprint*
[9] Kirczenow G 1989 *Phys. Rev. Lett.* **62** 2993
[10] Wharam D A, Ekenburg U, Pepper M, Hasko D G, Ahmed H, Frost J E F, Ritchie D A, Peacock D C and Jones G A C 1989b *Phys. Rev.* B 6283
[11] Lee K, Shur M S, Drummond T J, and Morkog H 1983 *J. Appl. Phys.* **54** 6432
[12] Laux S E, Frank D J and Stern F 1988 *Surf. Sci.* **196** 101
[13] Kittel C 1986 *Introduction to Solid State Physics* (New York: Wiley) p 196
[14] Rauh A, Wannier G H and Obermair G 1974 *Phys. Status Solidi* b **63** 215